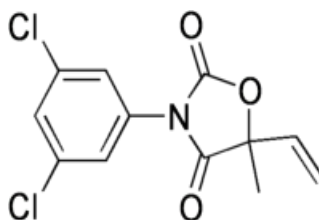


I. C₆₀-functionalized MWCNT based sensor for sensitive detection of endocrine disruptor vinclozolin in solubilized system and wastewater

1.1 Objectives

Vinclozolin (VZ) is an agricultural fungicide widely used in the United States of America and the European Union (50,000 kg/year) for the control of fungal spore germination in grapes, strawberries and various vegetables [1]. VZ (Scheme 1) has been identified as an anti-androgenic endocrine disruptor that produces malformations related to androgen inhibition in mammals [2] and birds [3]. In mammals VZ disrupts male steroid profiles and alters female gonadal condition in adults cause endocrine disruption [4].

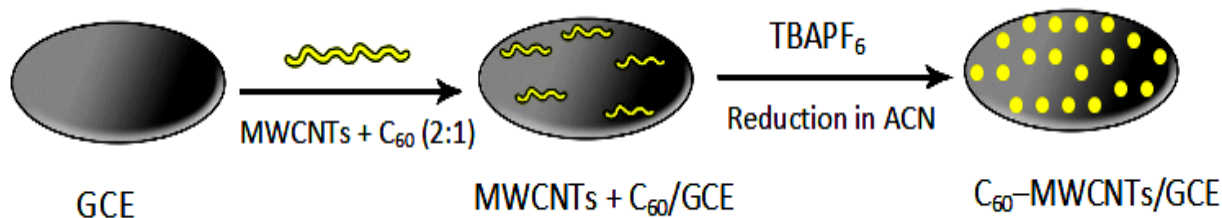


Scheme 1: Structure of vinclozolin

The microfabrication of voltammetric sensors is a field of paramount importance in the modern electrochemistry especially due to the various application possibilities of modified electrodes [5, 6]. In the present work, we compare the sensitivity of three electrodes, glassy carbon electrode (GCE), multi-walled carbon nanotubes modified glassy carbon electrode (MWCNTs/GCE) and fullerene-functionalized multi-walled carbon nanotubes modified glassy carbon electrode (C₆₀-MWCNTs/GCE) for the detection of the endocrine disruptor VZ in a solubilized system (CTAB) and wastewater. The results showed that the composite film of C₆₀-MWCNTs on GCE is more sensitive for the detection of vinclozolin compared to bare GCE and MWCNTs/GCE.

1.2 Fabrication, characterization and electrocatalytic effect of C₆₀-MWCNTs/GCE sensor

The fabricated sensor was characterized by scanning electron microscopy and electrochemical impedance spectroscopic techniques and this fabricated sensor shows high electrocatalytic activity for the detection of VZ.



Scheme 2: Fabrication of C₆₀-MWCNTs/GCE sensor

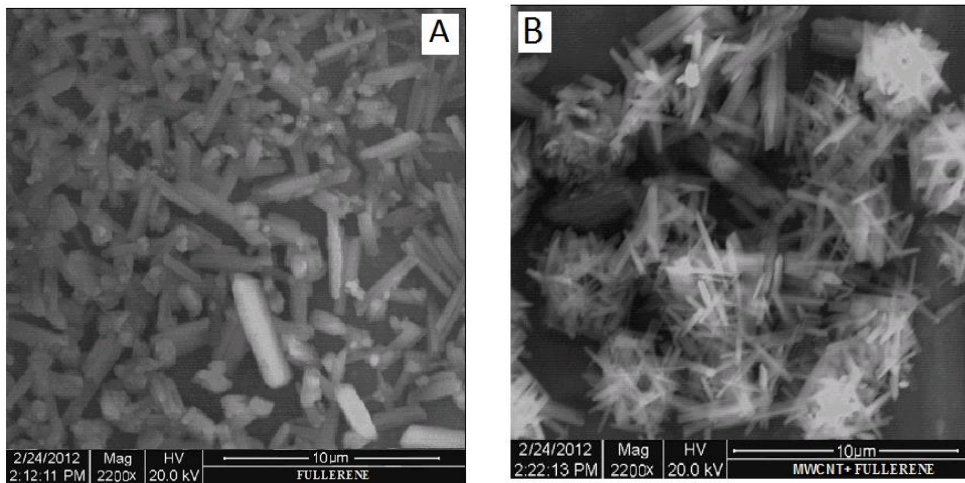


Figure 1: Scanning electron micrograph of (A) C_{60} /GCE, and (B) C_{60} -MWCNTs/GCE

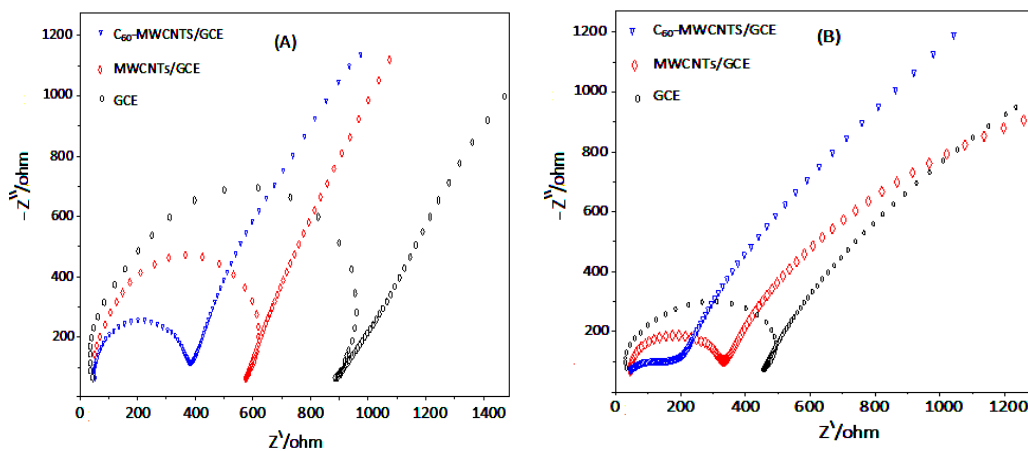


Figure 2: (A) Nyquist plots obtained at GCE (curve black), MWCNTs/GCE (curve red) and C_{60} -MWCNTs/GCE (curve blue) in 1.0 mM $K_3[Fe(CN)_6]$; (B) Nyquist plots obtained at GCE (curve black), MWCNTs/GCE (curve red) and C_{60} -MWCNTs/GCE (curve blue) in 0.25 mM VZ.

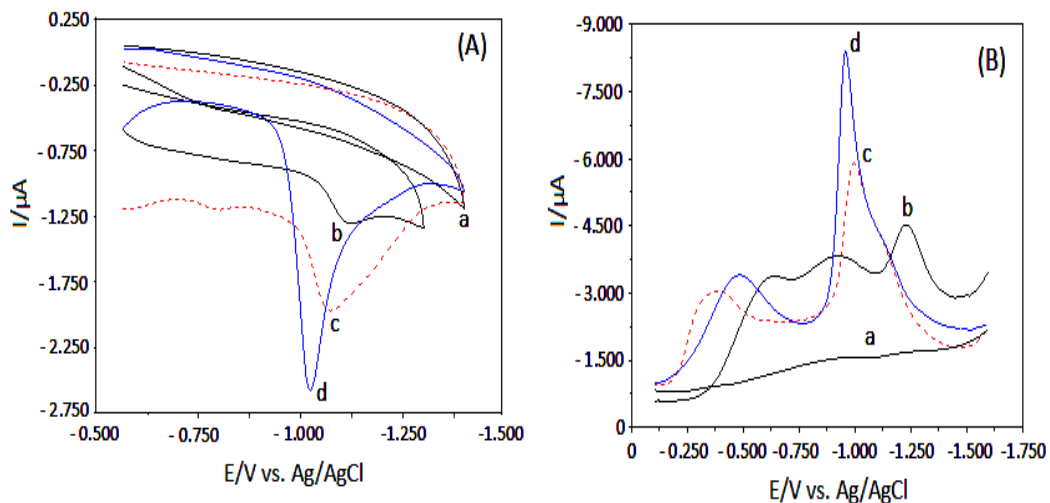


Figure 3: Electrocatalytic effect of fabricated sensor towards the reduction of vinclozolin (A) Cyclic voltammograms, Blank (curve a), 3.64 μM VZ at GCE (curve b), at MWCNTs/GCE (curve c) and at C_{60} -MWCNTs/GCE (curve d), scan rate 30 mVs^{-1} . (B) Squarewave voltammograms Blank (curve a), 3.64 μM VZ at GCE (curve b), at MWCNTs/GCE (curve c) and at C_{60} -MWCNTs/GCE (curve d).

Squarewave voltammograms obtained with increasing concentration of VZ showed that the peak current increased linearly with increasing concentration in the range of 2.54 to 8.75 μM and the detection limit (LOD) was estimated as $3s/m$ and found to be $0.091\mu\text{M}$ and the quantitation limit (LOQ) was calculated as $10s/m$ and found to be $0.3\mu\text{M}$, with s representing the standard deviation of the peak currents ($n = 3$) and m is the slope of the calibration curve (Figure 4).

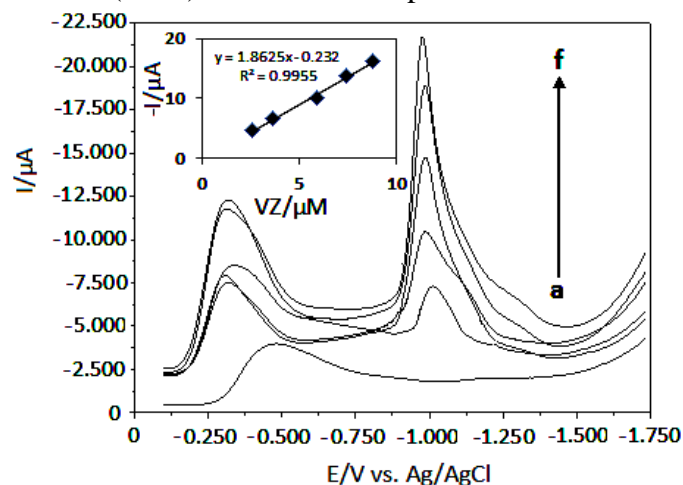


Figure 4: Linearity of the squarewave voltammetric peak current of VZ at different concentrations on C_{60} -MWCNTs/GCE (pH 9.0); (a) Blank (b) 2.54 (c) 3.64 (d) 5.86 (e) 7.43 (f) 8.75 μM .

1.3 Conclusion

A versatile electrochemical sensor was developed for the detection of endocrine disruptor VZ in solubilized system of CTAB and its analytical performance was systematically and comparatively studied with MWCNTs-based GCE and bare GCE. The use of solubilized system (CTAB) adds a beneficial and new dimension to electrode behaviour investigations, as polar surfactants being amphiphilic molecules tend to adsorb at the interface between the electrode and the solution which results in significantly change in the redox potential, charge transfer coefficients and diffusion coefficients, enhancing the electroanalytical response and hence lowers the detection limit. The obtained results shows that a nanocomposite film of C_{60} -MWCNTs provided significant advantages over MWCNTs/GCE and GCE in achieving faster response, excellent electrocatalytic activity, better repeatability, lower background current and low detection limit which could be attributed to its larger specific surface area and greater electron transfer rate. A typical sample analysis took less than 5 min for the detection of VZ. Hence, an excellent approach towards the development of a novel C_{60} -MWCNTs sensor has been presented which would become a pragmatic tool for convenient detection of endocrine disruptor VZ in wastewater. The main advantage of this new method is the use of less hazardous surfactant media in place of organic solvents which leads to the path of green technology.

1.4 References

- [1] A. Hossaini, J. J. Larsen J. C. Larsen, *Food Chem. Toxicol.* 38 (2000)319.
- [2] P.D. Darbre, J. R. Byford, L. E. Shaw, S. Hall, N. G. Coldham, G. S. Pope, *J. Appl. Toxicol.* 23 (2003) 43.
- [3] J. P. Routledge, J. Odum, J. P. Sumpter, *Toxicol. Appl. Pharm.* 153 (1998) 12.
- [4] P. W. Harvey, D. J. Everett, *J. Appl. Toxicology* 24 (2004) 1.
- [5] M. Thomassin, E. Cavalli, Y. Guillaume, C. Guinchard, *J. Pharm. Biomed. Anal.* 15 (1997) 831.
- [6] K. D. Altria, J. Bestford, *J. Capillary Electrophor.* 3 (1996) 13.

II. Fullerene-C₆₀ sensor for ultra– high sensitive detection of bisphenol – A and its treatment by green technology

2.1 Objectives

Bisphenol–A (BPA) is an estrogenic environmental toxin widely used in the production of plastics and ubiquitous human exposure to this chemical has been proposed to be a potential risk to public health which produce a broad range of adverse effects, including impaired brain development, sexual differentiation, behavior, and immune function, which could extend to future generations [1–3]. The detection and treatment of bisphenol A (BPA) in wastewater (WW) and wastewater sludge (WWS) is of major interest to assess the endocrine activity of effluent discharged into the environment. Among electrochemical sensors, no sensor based on fullerene modified glassy carbon electrode has been reported for the determination of BPA. Therefore, this paper describes a simple method based on immobilization of fullerene on glassy carbon electrode (GCE) for the determination of trace amounts of BPA. The fabricated sensor showed an excellent electrocatalytic activity in lowering the anodic overpotential and remarkable enhancement of the anodic current of BPA compared with the electrochemical performances obtained at a GCE.

The fullerene-C₆₀ sensor for the detection of BPA is fabricated by preparation of stock solution of C₆₀ in CH₂Cl₂ (150 μM) and then known volume (25 μL) of this solution was adsorbed onto the surface of the clean (polished with PK-4 polishing kit, BASi MF-2060) and dried GCE using a microsyringe and dried under room temperature. The C₆₀ film formed was then reduced in 1.0 mol/L KOH in the potential range 0.0 to -1.5 V at 10 mVs⁻¹ [4]. The phosphate buffer of pH 8.0 was taken in another cell and the electrode surface was equilibrated in it by cyclic scanning in the potential range of 550 mV to -50 mV (vs. Ag/AgCl) at a scan rate of 20 mVs⁻¹ for 20 minutes under a nitrogen atmosphere. Then modified sensor was stored at + 4⁰C till use.

2.2 Fabrication, characterization and electrocatalytic effect of C₆₀/GCE sensor

The fabricated fullerene-C₆₀ sensor was characterized and performed by scanning electron microscopy, electrochemical impedance spectroscopy (EIS) and voltammetry cyclic (CV), square wave (SWV) and differential pulse (DPV) voltammetry (Figure 1).

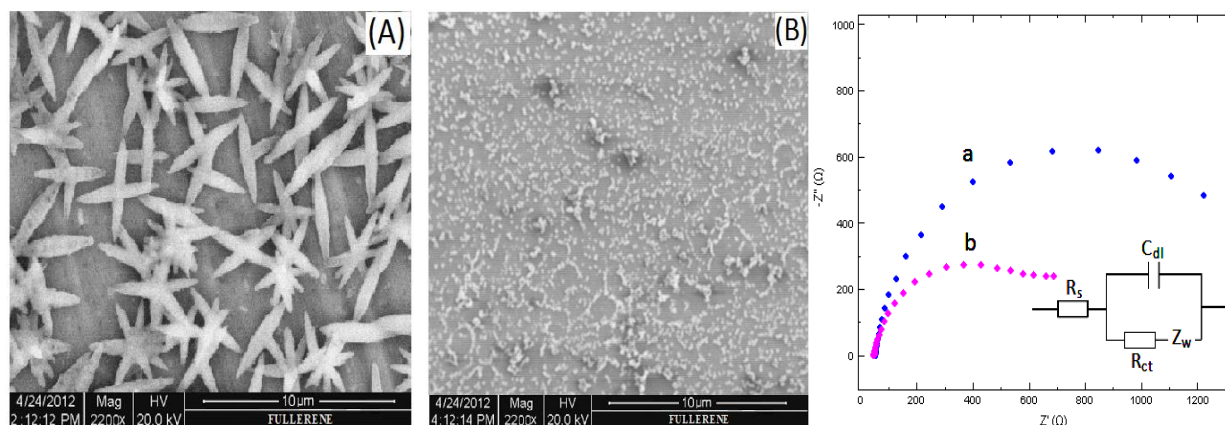


Figure 1: Scanning electron micrographs of C₆₀/GCE before (A) and after (B) reduction in KOH; Nyquist plots (right side) obtained at GCE (curve a) and C₆₀/GCE (curve b) in 1.0 mM K₃[Fe(CN)₆].

The performance of C_{60}/GCE sensor towards $0.19\mu\text{M}$ BPA oxidation shows that the fabricated sensor has significant catalytic effect on the BPA oxidation leading to a decrease of the overpotential and an enhancement of the peak current (Figure 2).

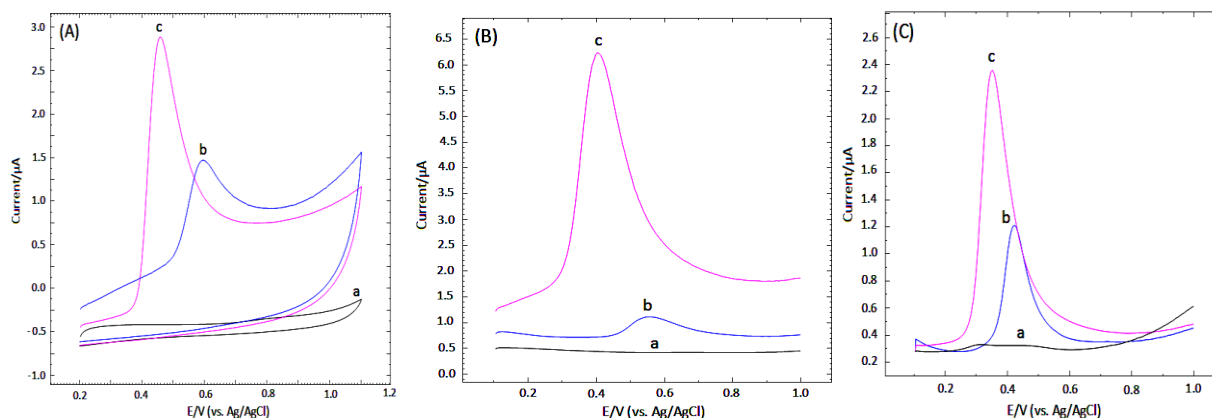


Figure 2: Electrochemical effect of C_{60}/GCE on $0.19\mu\text{M}$ BPA voltammograms A (CV; scan rate 10 mVs^{-1}), B (SWV) and C (DPV) at (a) blank, (b) bare glassy carbon electrode (c) C_{60}/GCE

The calibration plot of concentration versus peak current was found to be linear over the range 74 nM to $0.23\text{ }\mu\text{M}$ expressed by linear calibration equation: $i_p/\mu\text{A} = 42.584(\text{BPA}) - 0.2192$; $r^2 = 0.995$ (Figure 3 A). The detection limit (LOD) was estimated as $3s/m$ and found to be 3.7 nM , with s representing the standard deviation of the peak currents ($n = 3$) and m is the slope of the calibration curve.

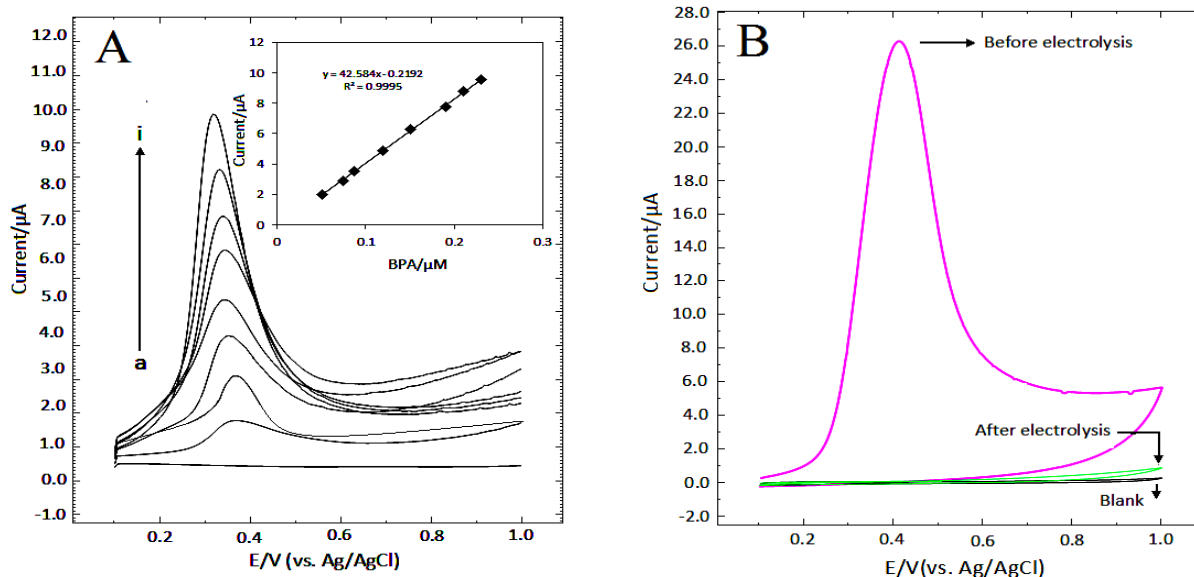


Figure 3: (A) Linearity of squarewave voltammetric peak current of different concentrations of BPA (a) Blank (b) 74 nM (c) 87 nM (d) $0.12\text{ }\mu\text{M}$ (e) $0.15\text{ }\mu\text{M}$ (f) $0.19\text{ }\mu\text{M}$ (g) $0.21\text{ }\mu\text{M}$ and (i) $0.23\text{ }\mu\text{M}$; (B) Cyclic voltammetric response of BPA at C_{60}/GCE before and after bulk electrolysis.

The treatment of wastewater containing BPA by green technology by charging BASi cell with 15 mg (1.3 mM) BPA in 50 mL wastewater (provided by the Aquafin Water Treatment Company located in Antwerp, Belgium) containing phosphate buffer pH 8.0 . The estrogenic activity of the

BPA is due to the structural resemblances with the estrogenic hormones which is mainly occurs due to the presence of the phenolic functional groups [5, 6]. During bulk electrolysis the OH groups of the BPA gets completely oxidized and results in the formation of quinone and hence BPA lost its estrogenic activity and this result in treatment of matrix such as wastewater containing BPA (Figure 3B). This method does not involve any hazardous chemicals or any sample extraction procedure prior to the analysis and thus this treatment method is a form of green technology.

2.3 Conclusions

A highly enhancing sensing platform based on fullerene fabricated electrochemical sensor C60/GCE was established for the trace detection of endocrine disruptor BPA. The fabricated sensor showed an excellent electrocatalytic activity in lowering the anodic overpotential and remarkable enhancement of anodic current of BPA compared with electrochemical performances obtained at GCE. The kinetic parameters such as charge transfer coefficient (α), electrode surface area (A) and diffusion coefficient (D) for the oxidation of BPA is determined using the proposed method. The treatment of the wastewater by bulk electrolysis cell leads to the path of green technology. The simplicity of the fabrication procedure, ease of the detection step and good reproducibility of the proposed method open up increasing possibility for the future development of fullerene sensors for environmental applications.

2.4 References

- [1] A. Krishnan, P. Stathis, S. Permuth, L. Tokes, D. Feldman, *Endocrinology* 132 (1993) 2279–2286.
- [2] P. Palanza, L. Gioiosa, F. S. vom Saal, S. Parmigiani *Environ. Res.* 108 (2008) 150–157.
- [3] J. Y. Youn, H. Y. Park, J. W. Lee, I. O. Jung, K. H. Choi, K. Kim, K. H. Cho, *Arch. Pharm. Res.* 25 (2002) 946–953.
- [4] M. Csiszar, A. Szucs, M. Tolgyesi, A. Mechler, J. B. Nagy, M. Novak, *J. Electroanal. Chem.* 497 (2001) 69–74.
- [5] J. C. Gould, L. S. Leonard, S. C. Maness, B. L. Wagner, K. Conner, T. Zacharewski, S. Safe, D. P. McDonnell, K. W. Gaido, *Mol. Cell. Endocrinol.* 142 (1998) 203–214
- [6] G. G. Kuiper, J. G. Lemmen, B. Carlsson, J. C. Corton, S. H. Safe, P. T. Van Der Saag, B. van der Burg, *Endocrinology* 139 (1998) 4252–4263.

III. Rapid microwave synthesis of high aspect-ratio ZnO nanotetrapods for swift bisphenol – A

3.1 Objectives

The introduction of the bottom-up model as a potential option of miniaturization for technological development led to the precise investigation of methods to develop semiconductor nanostructure as the building blocks of functional nanodevices. Essential to the paradigm is the capability to fabricate and tailor nanostructures into a particular morphology and preferred size to attain the desired properties and functionalities, which has been proficient by producing crystals in a variety of fascinating shapes [1, 2]. Among them, ZnO has tremendous ability to grow into different shapes and morphologies. We have recently developed microwave synthesis due to its rapid, high crystallinity, reproducibility and mass production for high aspect-ratio ZnO nanotetrapods.

Bisphenol A (BPA) is EDC widely used in the plastic industry as a monomer for producing epoxy resins and polycarbonate. In our life, BPA is ubiquitous since it can be released into the environment from bottles, packaging, and landfill leachates as well as plastics plants [3–5]. BPA is non-biodegradable and highly resistant to chemical degradation, so that the concentration of BPA in the environmental is frequently high [6]. Therefore, it has become very essential to establish sensitive method for the determination of BPA.

In the present report ZnO nanotetrapods were synthesized using microwave technique and the growth of these nanotetrapods occurs by vaporizes zinc and condenses in supersaturated air into a tiny Zn clusters with few atoms. With elevated temperature, these clusters oxidizes quickly because of ambient oxygen and results into the formation of tiny ZnO nuclei. These nuclei further grow because of the condensation of more Zn and O atoms and attain instability and crumple to form bigger crystal structure. Electrochemical sensors have great potential for environmental monitoring because of their portability, field-deploy ability, excellent sensitivity (in low ppb levels), automation, short analysis time, low power consumption and inexpensive equipment. Among electrochemical sensors, no sensor based on zinc oxide nanotetrapods modified glassy carbon electrode (T-ZnO/GCE) has been reported for the detection of BPA. Therefore, in this paper we have illustrated the fabrication of a novel sensor for the trace detection of BPA due to its immense importance. This high aspect ratio ZnO nanotetrapods based electrochemical sensor showed an excellent electrocatalytic activity in terms of remarkable enhancement of the anodic current of BPA and lowers the detection limit and compared the performance with various reported electrochemical sensors elsewhere.

Before sensor fabrication, the GCE surface was polished with PK-4 polishing kit, BASi MF-2060 successively followed by rinsing thoroughly with redistilled deionized water until a mirror like finish was obtained. It was then dipped in a beaker containing 0.2 mol/L H_3PO_4 solutions to remove the adhered powder, rinsed with distilled water and dried at room temperature for 10–15 minutes. Stock solution of zinc oxide nanotetrapods (1.0 mg/mL) was prepared in 50% dimethyl sulfoxide (DMSO) by ultrasonication for 30 minutes. Then 10 μ L of this solution was adsorbed onto the surface of GCE using a microsyringe and dried under IR lamp. Then modified sensor was stored at + 4⁰C till use.

3.2 Results and Discussion

3.2.1 Characterization of synthesized ZnO nanotetrapods and T-ZnO/GCE sensor

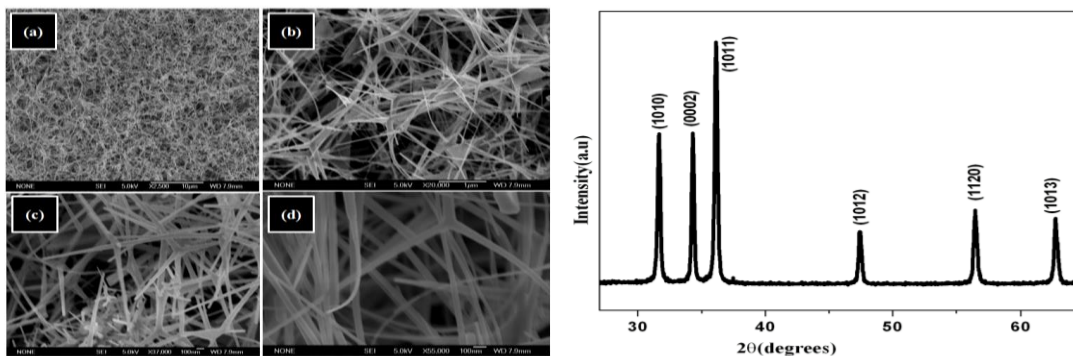


Figure 1: (a-d) Low and high magnification FESEM and HRETEM images of ZnO nanotetrapods; XRD pattern of ZnO nanotetrapods synthesized by microwave evaporation.

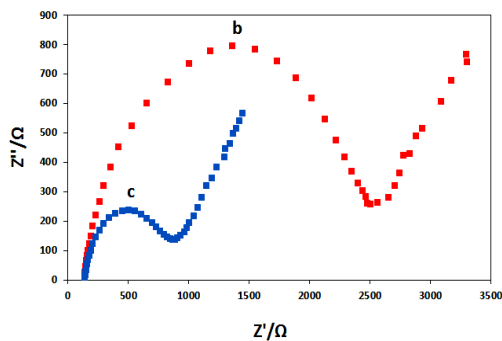


Figure 2: Nyquist plots obtained at GCE (curve b) and T-ZnO/GCE (curve c) in 1.0 mM $K_3[Fe(CN)_6]$

3.2.2 Electrocatalytic oxidation of BPA at T-ZnO/GCE sensor

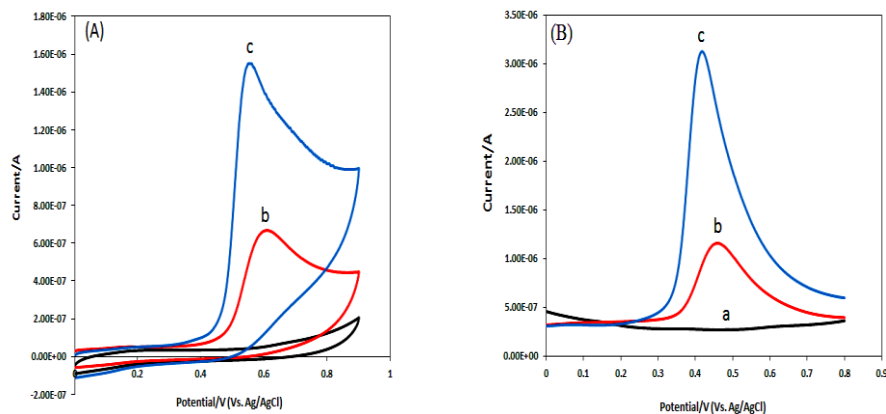


Figure 3: (A) Cyclic voltammetric behavior (a) Blank, and (b) 42.5 nM BPA at GCE, (c) 42.5 nM BPA at T-ZnO/GCE; scan rate 20 mVs^{-1} . (B) Squarewave voltammetric behaviour (a) Blank, and (b) 42.5 nM at GCE, (c) 42.5 nM BPA at T-ZnO/GCE; (frequency (f) = 25 Hz and pulse amplitude (ΔE_{sw}) = 50 mV).

3.2.3 Analytical application

Squarewave voltammograms obtained with increasing amounts of BPA showed that the peak current increased linearly with increasing concentration over the range 12.4 nM to 1.2 μ M (Figure 4). The detection limit (LOD) estimated as $3s/m$ was found to be 1.5 nM and sensitivity was calculated as $10s/m$ found to be $5.0 \mu\text{A nM}^{-1} \text{cm}^{-2}$, with s representing the standard deviation of the peak currents ($n = 3$) and m is the slope of the calibration curve.

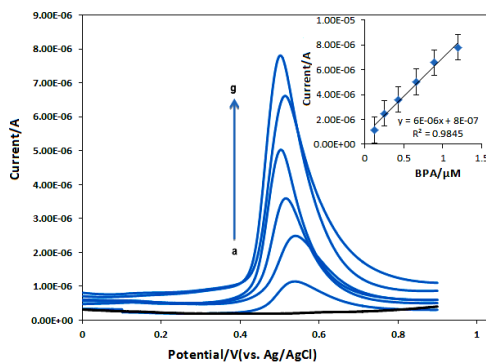


Figure 4: Linearity of squarewave voltammetric peak current of different concentrations of BPA at T-ZnO/GCE (a) Blank (b) 12.4 nM (c) 25.3 nM (d) 42.5 nM (e) 65.7nM (f) 89.2 nM (g) 1.2 μ M; Inset a calibration graph represents the variation of current with the concentration of BPA. The error bars shows the standard deviation obtained for three separate experiments.

3.3 Conclusions

ZnO nanotetrapods were synthesized by very fast highly reproducible microwave synthesis method in grams quantity. FESEM investigation confirmed that each tetrapod has four arms and they originated from the one centre. The diameter of arms was larger at the base and smaller at the tips. Comprehensive structural examination revealed that these nanotetrapods are single crystalline and wurtzite hexagonal crystal structure. The obtained results shows that a nano film of T-ZnO provided significant advantages over GCE in achieving faster response, excellent electrocatalytic activity, better repeatability, lower background current and low detection limit of BPA which could be attributed to its larger specific surface area and greater electron transfer rate. The simplicity of the fabrication procedure opens up increasing possibility for the future development of T-ZnO sensors for environmental applications.

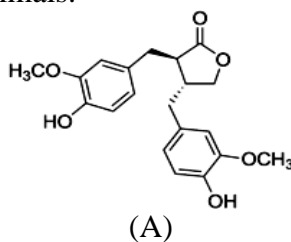
3.4 References

- [1] C. L. Choi, A. P. Alivisatos, *Annu. Rev. Phys. Chem.* 61(2010) 369.
- [2] S. Kumar, T. Nann, , *Small* 2 (2006) 316.
- [3] J.Y. Hu, T. Aizawa, S. Ookubo, *Environ. Sci. Technol.* 36 (2002) 1980.
- [4] D.W. Kolpin, E.T. Furlong, M.T. Meyer, E.M. Thurman, S.D. Zaugg, L.B. Barber, H.T. Buxton, *Environ. Sci. Technol.* 36 (2002) 1202.
- [5] B. Hileman, *Chem. Eng. News* 81 (2003) 40.
- [6] X. L. Jin, G. B. Jiang, G. L. Huang, J. F. Liu, Q. F. Zhou, *Chemosphere* 56 (2004) 1113.

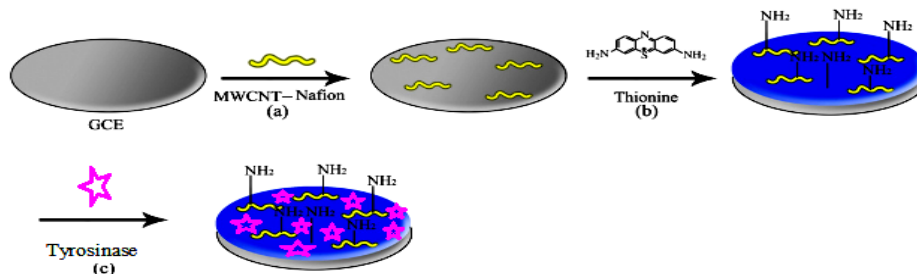
IV. A biosensor fabricated by incorporation of redox mediator into carbon nanotube/nafion composite for tyrosinase immobilization: detection of matairesinol an endocrine disruptor

4.1 Objectives

Plant-derived phytoestrogens are a group of such chemicals which are stereochemically similar to the hormone 17- β -estradiol [1]. They have other possible effects on some enzymes, inhibiting steroid metabolism, anti-proliferative and anti-angiogenic processes, protein tyrosine kinase inhibition and other biological effects have been described [2]. Matairesinol (A) is a plant lignin found mainly in flax seeds and rye and has estrogen-like structure [3]. In gastrointestinal tract matairesinol is converted into metabolite enterodiol which is known to have estrogenic properties [4]. Therefore reliable data on the phytoestrogen matairesinol is necessary to assess the health implications on humans and other animals.



Literature survey reveals the coulometric electrode array detection for determination of matairesinol in flax seeds with detection limit of $5 \mu\text{g g}^{-1}$ [5]. All reported techniques for the detection of EDCs are reaching high accuracy with low detection limits, but are expensive, time-consuming and require the use of highly trained personnel. The fabrication of biosensors has generated tremendous interest in this area. In the present work, the deliberate combination of thionine, CNTs and nafion for tyrosinase immobilization is very interesting. It has been recently reported that CNTs showed a strong tendency to adsorb thionine molecules through donor-acceptor interaction and also π - π stacking force between these two kinds of conjugated frames [6]. There is strong interaction between any of two among the three materials (ion-exchange process between thionine and nafion, strong adsorption of thionine by CNTs and wrapping and solubilizing of CNTs with nafion), which will result in the homogenization of the three materials that provides efficient immobilization matrix for tyrosinase enzyme by increasing the electron transfer with the significant decrease of high overpotential. Our strategy is to immobilize the enzyme into an electrically conductive matrix of carbon nanotubes, thionine and nafion which potentially reduces the distance from the redox-centre of tyrosinase to the CNT that promote faster electron transfer.



Scheme 1: Fabrication of the biosensor

4.2 Results and Discussion

4.2.1 Characterization of biosensor

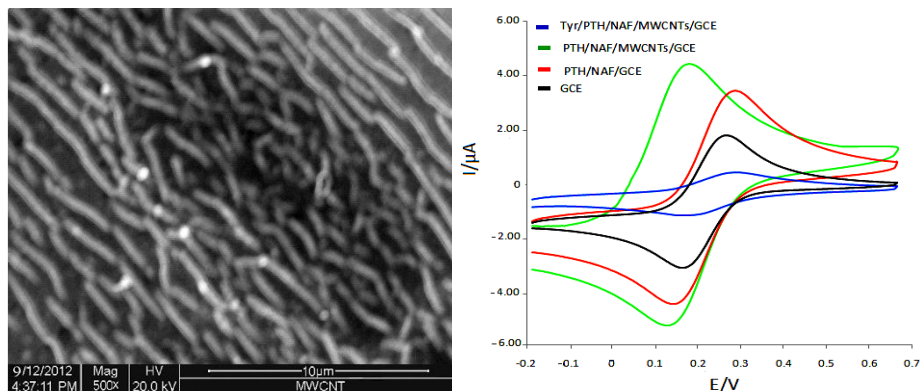


Figure 1: Scanning electron micrographic image of NAF/MWCNTs/GCE; Cyclic voltammograms of 1.0 mM $K_3[Fe(CN)_6]$ in 0.1M KCl, scan rate of 20 mVs^{-1} at different modified electrodes; GCE, (—), PTH/NAF/GCE (—), PTH/NAF/MWCNTs/GCE (—) and Tyr/PTH/NAF/MWCNTs/GCE (—).

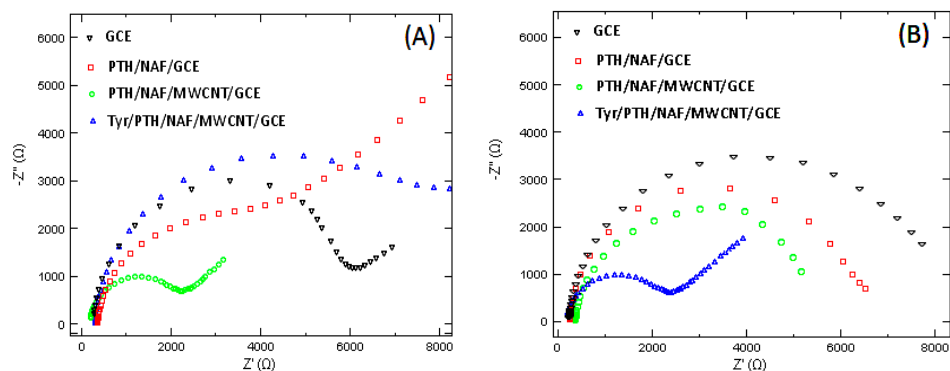


Figure 2: (A) Nyquist plot of 1.0 mM $K_3[Fe(CN)_6]$ in 0.1M KCl at different modified electrodes GCE, (▾), PTH/NAF/GCE (▣), PTH/NAF/MWCNTs/GCE (▣) and Tyr/PTH/NAF/MWCNTs/GCE (▴).

4.2.2 Electrocatalytic oxidation of matairesniol

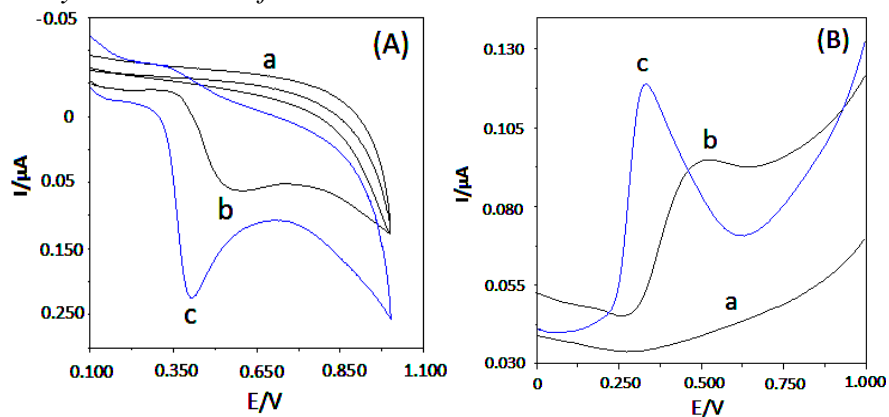


Figure 3: (A) Cyclic voltammetric behaviour (a) Blank, and (b) 18 nM matairesniol at GCE, (c) 18 nM matairesniol at Tyr/PTH/NAF/MWCNTs/GCE; scan rate 20 mVs^{-1} . (B) Squarewave voltammetric behaviour (a) Blank, and (b) 18 nM at GCE, (c) 18 nM at Tyr/PTH/NAF/MWCNTs/GCE.

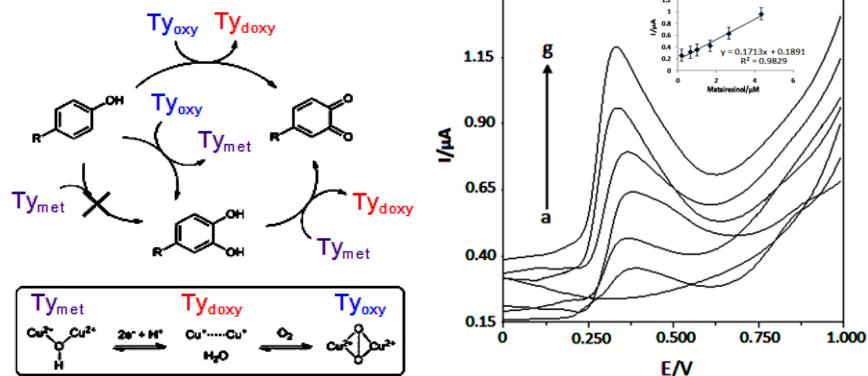


Figure 4: Mechanism of the electrode reaction; Linearity of squarewave voltammetric peak current of matairesinol at different concentrations Tyr/PTH/NAF/MWCNTs/GCE (pH 7.0); (a) Blank (b) 18 nM (c) 65.3 nM (d) 98.4 nM (e) 1.68 μM (f) 2.65 μM (g) 4.33 μM. The error bars represents standard deviation from three separate experiments.

4.2.3 Linearity range and detection limit

Squarewave voltammograms of matairesinol at Tyr/PTH/NAF/MWCNTs/GCE showed that the peak current increased linearly with increasing concentration (Figure 4). The linearity evaluated by linear regression analysis was calculated by least square regression method [7]. The linearity was obtained over the concentration range 18 nM to 4.33 μM and the linear regression equation is $I_p/\mu A = 0.1713 (\mu M) + (0.1813)$; $r^2 = 0.9829$ ($n = 3$). The detection limit (LOD) estimated as $3s/m$ is found to be 3.7 nM with s representing the standard deviation of the peak currents ($n = 3$) and m is the slope of the calibration curve.

4.3 Conclusions

In the present work, through a simple route by incorporating redox mediator thionine into the CNTs/nafion composite matrix for immobilization of tyrosinase is a new electrochemical sensing platform, due to the ion-exchange ability of nafion and the strong adsorption of CNTs. Benefiting from the coupling of the antifouling/discriminative properties of nafion with three-dimensional electronic conductivity of CNTs and highly intimate contact with thionine, the integrated thionine and CNTs/nafion composite film shows a stable and high matrix which enhances the electrocatalytic response of tyrosinase toward the oxidation of matairesinol at a much lower potential. The composite electrode showed an excellent electrocatalytic activity in lowering the anodic overpotential and remarkable enhancement of the anodic current of matairesinol if compared with the electrochemical performances obtained at a GCE. The kinetic parameters such as standard rate constant (K_0) and the diffusion coefficient (D_0) for the oxidation of matairesinol were determined using the proposed method. The fabricated biosensor has been successfully used for detection of matairesinol with remarkable properties such as fast response, broad linear range, good reproducibility, acceptable stability and low detection limit.

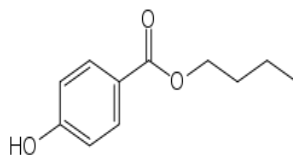
4.4 References

- [1] Y. Zhang, J. L. Zhou, Water Res. 39 (2005) 3991.
- [2] M. Fitzpatrick, J. Agric. Food Chem. 46 (1998) 3396.
- [3] H. Adlercreutz, W. Mazur, Ann. Med. 29 (1997) 95.
- [4] S. Heinonen, T. Nurmi, K. Liukkonen, K. Poutanen, K. Wa ha la, T. Deyama, S. Nishibe, H. Adlercreutz, J. Agric. Food Chem. 49 (2001) 3178.
- [5] T. Kraushofer, G. Sontag, J. Chromatogr. B. 777(2002) 61.
- [6] Q.W. Li, J. Zhang, H. Yan, M.S. He, Z.F. Liu, Carbon 42 (2004) 287.
- [7] E. J. Laviron, J. Electroanal. Chem. 112 (1980) 11.

V. Polycyclodextrin and carbon nanotubes as composite for tyrosinase immobilization and its superior electrocatalytic activity towards butylparaben

5.1 Objectives

The European Commission listed in June 2012 during the conference on “Endocrine Disruptors: Current challenges in science and policy” parabens as Category 1 priority endocrine disruptor substances, based on evidence that they interfere with hormone function. Parabens are designed as esters of p-hydroxybenzoic acid and are extensively used as antimicrobial preservatives in food ingredients, cosmetic consumer products as well as pharmaceutical preparations. The parabens present in these products are continuously released into the aquatic media through domestic wastewater. Therefore, there is growing concern in relation to their potential long-term effects on humans and wild life [1] for example incidence of breast cancer [2] and negative influence on the male reproductive function (testosterone synthesis) confirmed by Rodents exposure to parabens [3] are listed.



[A]

Various techniques are available for parabens detection such as high performance liquid chromatography [4], capillary electrochromatography [5], gas chromatography [6], flow injection system combined with chemiluminescence [7], solid phase extraction (SPE) [8] and supercritical fluid extraction (SFE) [9]. Although these techniques have high accuracy with low detection limits, they are expensive, time-consuming and due to the complexity of the environmental matrices, pre-concentration of the samples is required for the analysis [10]. In the present work, our strategy is to embed Tyr in a matrix of polycyclodextrin and CNTs. This is the first study for the bio-electrochemical detection of butylparaben, an endocrine disruptor. The CDP was prepared as reported by cross-linking cyclodextrin under strongly alkaline conditions with epichlorohydrin [11]. The preparation of CDP was characterized by UV-Vis spectroscopy. Both CD (curve a) and CDP (curve b) (Figure 1) give an absorption band around $\lambda = 275$ nm. It was observed that the intensity of the absorption band of CDP was 25% higher compared to CD, indicates high absorption due to polymerization of CD to CDP. The biosensor was fabricated as shown in scheme 1.

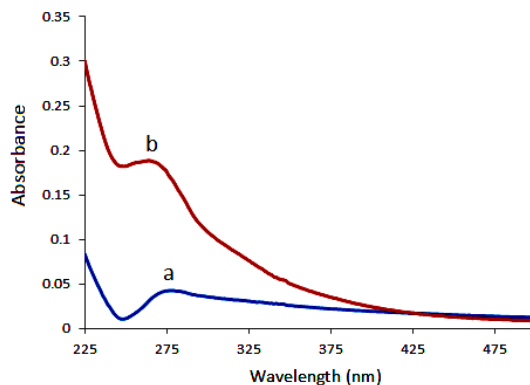
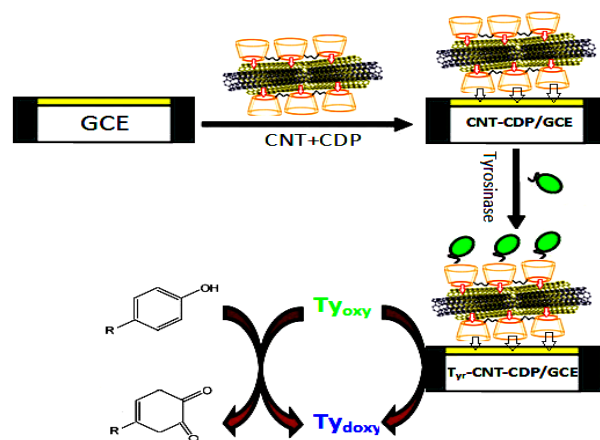


Figure 1: UV-Vis spectra of CD (curve a) and CDP polycyclodextrin (curve b)



Scheme 1: Fabrication of biosensor and mechanism of electrode reaction

5.2 Results and Discussion

5.2.1 Characterization and electrochemical performance of Tyr-CNT-CDP/GCE

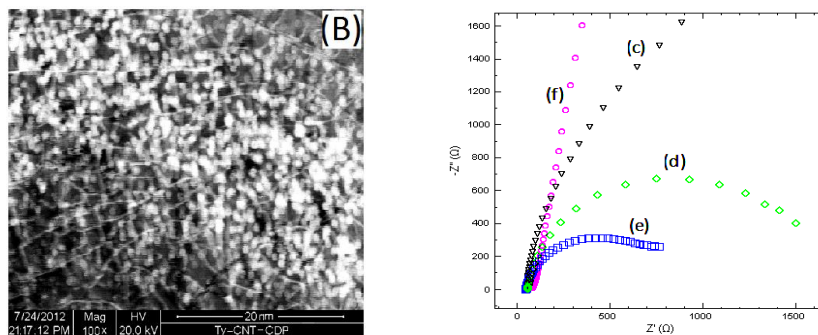


Figure 2: Scanning electron micrographs of CNT-CDP/GCE (A) and Tyr-CNT-CDP/GCE (B); Nyquist plots obtained at GCE (curve d), CDP-GCE (curve c), CNT-CDP/GCE (curve e) and Tyr-CNT-CDP/GCE (curve f) in 0.25 μM BP.

5.2.2 Electrochemical performance of Tyr-CNT-CDP/GCE for BP oxidation

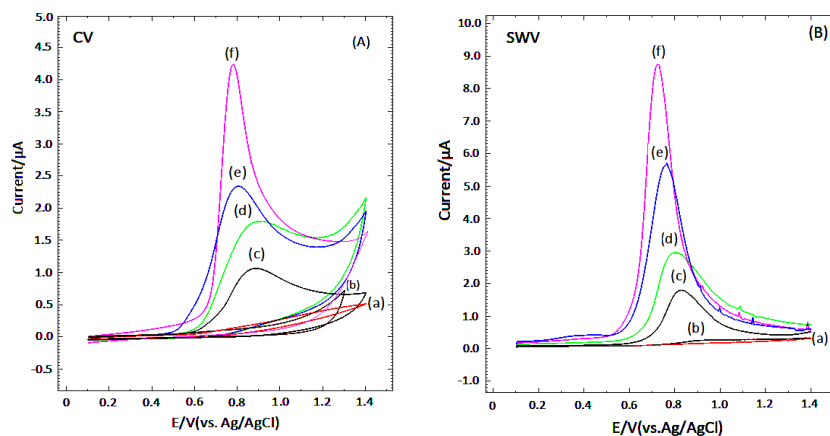


Figure 3: Comparison of cyclic (A) and squarewave (B) (frequency (f) = 25 Hz and pulse amplitude (ΔE_{sw}) = 50 mV) voltammograms in presence and absence of 10.24 μM BP at different types of electrodes: GCE blank (curve a), Tyr-CNT-CDP/GCE blank (curve b), GCE in BP (curve d), CDP/GCE in BP (curve c), CNT-CDP/GCE in BP (curve e) and Tyr-CNT-CDP/GCE in BP (curve f).

5.2.3 Effect of butylparaben concentration

It is observed from Figure 4 that the response current is linear with the BP concentration over the range from 2.1 to 35.4 μM , indicating that the enzyme catalytic reaction of Tyr is the first-order reaction. The detection limits was found to be 0.1 μM . Above a BP concentration value of 35 μM , the enzyme reaction shows a transition from first to zero-order showing a typical Michaelis–Menten kinetic mechanism. The apparent Michaelis-Menten constant (K_M^{app}) according to the electrochemical version of the Lineweaver–Burk equation [12]: $1/i_{\text{ss}} = (K_M^{\text{app}}/i_{\text{max}}) (1/c) + (1/i_{\text{max}})$ which gives the K_M^{app} value of 25.82 μM .

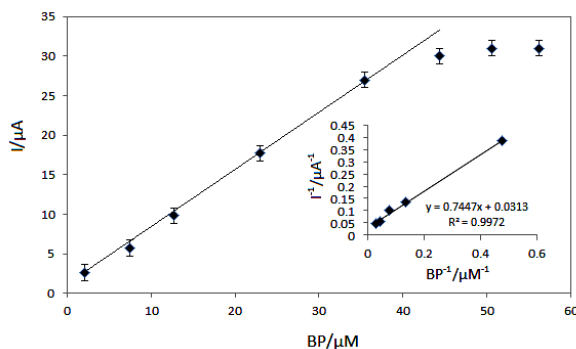


Figure 4: Calibration curve of Tyr–CNT–CDP/GCE for successive addition of BP in pH 7.0. Inset is the plot of the reciprocals of the steady-state current versus BP concentration.

5.3 Conclusions

In this study, the use of a nanocomposite consisting of carbon nanotubes and β -polycyclodextrin is investigated towards (1) the immobilization of tyrosinase and (2) the determination of butylparaben. Polycyclodextrin not only provides a good environment for enzyme immobilization but also increases the biocompatibility of the device. Since carbon nanotubes are highly conductive, the transferred electrons can easily percolate throughout a three dimensional matrix leading to a high efficiency of the bio-converted energy. Therefore by docking the carbon nanotubes near the enzyme activity centre and by choosing the appropriate reaction conditions to ensure the carbon nanotubes have good access to and large capacity of electrons, it was possible to maximize the performance of the functional hybrid materials as sensors. Hence, an excellent approach towards the development of a sensing device has been presented which would become a pragmatic tool for convenient detection of other endocrine disruptors in environmental matrices.

5.4 References

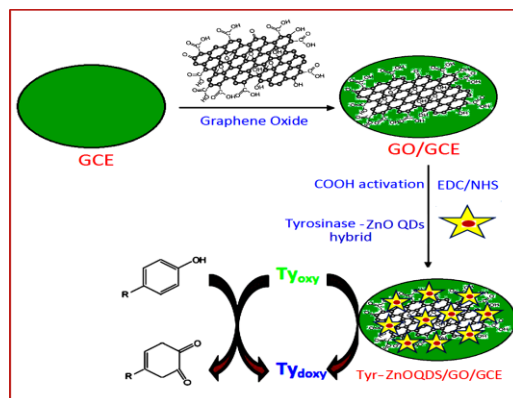
- [1] A. Hossaini, J. J. Larsen J. C. Larsen, *Food Chem. Toxicol.* 38 (2000)319.
- [2] P.D. Darbre, J. R. Byford, L. E. Shaw, S. Hall, N. G. Coldham, G. S. Pope, *J. Appl. Toxicol.* 23 (2003) 43.
- [3] S. Oishi, *Arch. Toxicol.* 76 (2002) 423.
- [4] M. Thomassin, E. Cavalli, Y. Guillaume, C. Guinchart, *J. Pharm. Biomed. Anal.* 15 (1997) 831.
- [5] K. D. Altria, J. Bestford, *J. Capillary Electrophor.* 3 (1996) 13.
- [6] P. Canosa, D. Perez-Palacios, A. Garrido-Lopez, M.T. Tena, I. Rodriguez, E. Rubi, R. Cela, *J. Chromatogr. A* 1161 (2007) 105.
- [7] R. K. Kobos, *Anal. Chem.* 6 (1987) 6.
- [8] S. Tuncagil, S. Varis, L. Toppare, *J. Mol. Catal. B: Enzym.* 64 (2010) 195.
- [9] R. Kazandjian, A. Klibanov, *J. Am. Chem. Soc.* 107 (1985) 5448.
- [10] C. B. Jacobs, M. J. Peairs, B. J. Venton, *Anal. Chim. Acta* 662 (2010) 105.
- [11] B. Ekberg, B. Sellergren, L. Olsson, K. Mosbach, *Carbohydr. Polym.* 10 (1989) 183.
- [12] R. A. Kamin, G. S. Willson, *Anal. Chem.* 52 (1980)1198 .

VI. A Graphene Oxide Amplification Platform Tagged with Tyrosinase-Zinc Oxide Quantum Dot Hybrids for the Electrochemical Sensing of Hydroxylated Polychlorobiphenyl

6.1 Objectives

Graphene is considered as the thinnest material in our universe which consists of flat monolayers with sp^2 -bonded carbon atoms tightly packed into a two-dimensional honeycomb lattice structure [1]. Graphene oxide (GO) is one of the most important derivatives of graphene having large surface area, excellent conductivity and strong mechanical strength and therefore they can be used for fabrication of novel electrochemical sensors and biosensors to facilitate the electron transfer reactions. In past decade semiconductor quantum dots (QDs) have gained a great deal of research interest due to their exciting size and quasi zero dimensional properties. Due to high isoelectric point (IEP 9.5) of ZnO QDs, the surface becomes positively charged in water, which is suitable for the adsorption of negatively charged proteins or enzymes with low IEP (*Tyr* IEP of 4.7– 5.0) [2]. Polychlorinated biphenyls (PCBs) are used as dielectric fluids in transformers and capacitors, as heat-transfer and hydraulic fluids [3]. The US Environmental Protection Agency (EPA) under the provisions of the Toxic Substances Control Act banned uses of PCBs in 1997. The European Community Directive 96/59/EC on the monitoring of PCBs provide regulations and treatment facilities of PCBs to be identified out by year 2010. The primary targets of PCBs are the endocrine (hormonal) and nervous systems causes low birth weight in children, neurobehavioral developmental delays, cognitive deficits, changes in production of thyroid hormones and altered reproductive system in males and females. In humans and wildlife animals, PCBs gets metabolized to hydroxylated PCBs (OH-PCBs) by cytochrome P450 enzyme-mediated phase oxidation mechanism [4].

It is well known that *Tyr* is a copper protein involved in two catalytic functions including ortho-hydroxylation of monophenols to o-diphenols in the presence of molecular oxygen (cresolase activity) and a two-electron oxidation of o-diphenols into o-quinones (catecholase activity) [5]. In the present study 2-hydroxy-2', 3', 4', 5, 5'-pentachlorobiphenyl (OH-PCBs) is taken as model which is a monophenolic compound. The present approach of biosensing OH-PCBs involves the use of graphene oxide amplification platform for the immobilization of a hybrid composed out of tyrosinase and ZnO QDs formed by electrostatic attraction between the positively charged ZnO QDs and the negatively charged tyrosinase. The procedure used for construction of the biosensing element is shown in scheme 1.



Scheme 1: Fabrication of biosensing element.

6.2 Results and Discussion

6.2.1 Characterization of graphene oxide and Tyr-ZnO hybrid

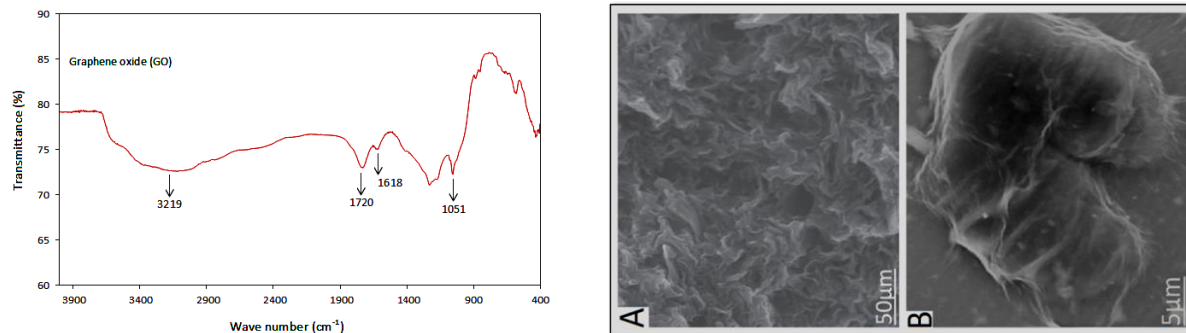


Figure 1: FTIR spectra of synthesized graphene oxide; scanning electron micrographs of graphene oxide at different magnifications ; (A) 50 μm and (B) 5 μm .

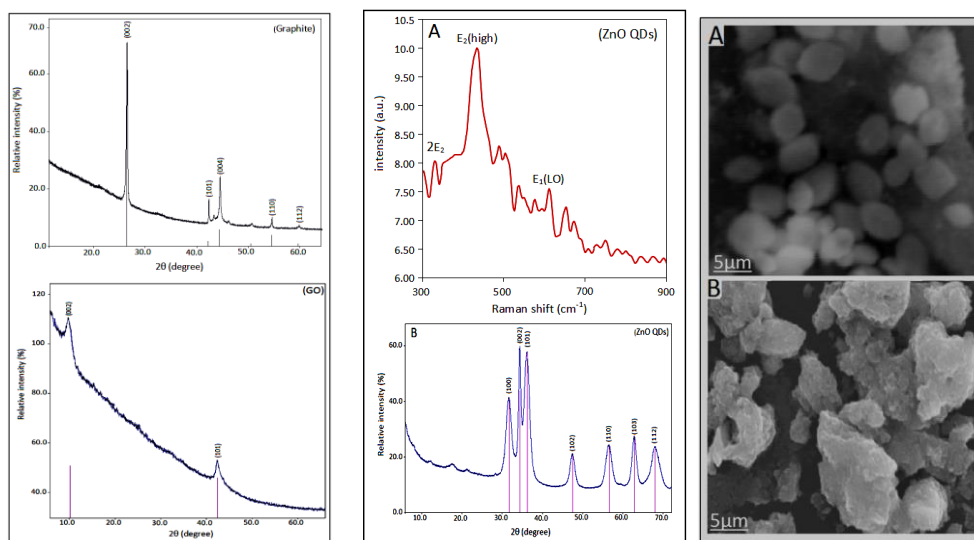


Figure 2 : XRD patterns of graphite and graphene oxide (GO); (A) Raman spectra of ZnO QDs (B) XRD patterns of ZnO QDs.; scanning electron micrographs of (A) ZnO QDs and (B) Tyr-ZnO hybrid.

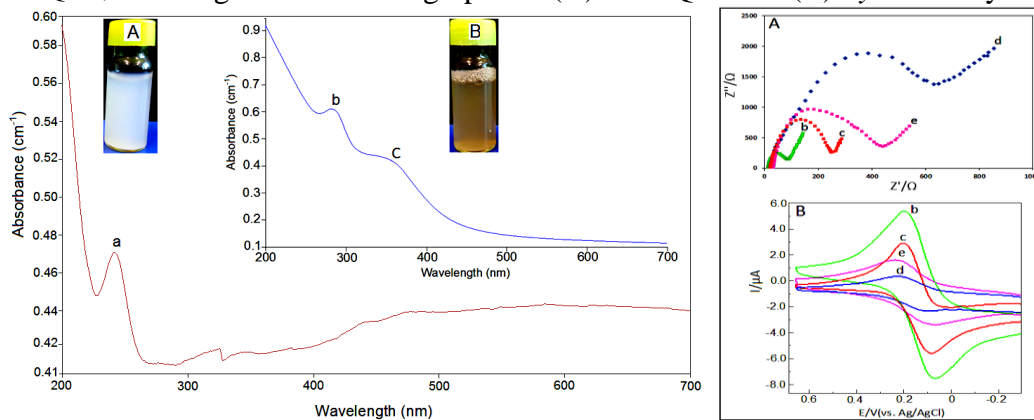


Figure 3: UV-Vis absorption spectra of (A) 1.0 mgmL^{-1} ZnO QDs and (B) 1.0 mgmL^{-1} Tyr-ZnO QDs hybrid; (A) Nyquist plots (B) Cyclic voltammety obtained at GCE (curve b), GO/GCE (curve c), Tyr/GO/GCE (curve d) and Tyr-ZnO/GCE (curve e) in 1.0 mM $\text{K}_3[\text{Fe}(\text{CN})_6]$.

6.2.2 Electrochemical performance of *Tyr*-ZnO/GO/GCE towards OH-PCBs

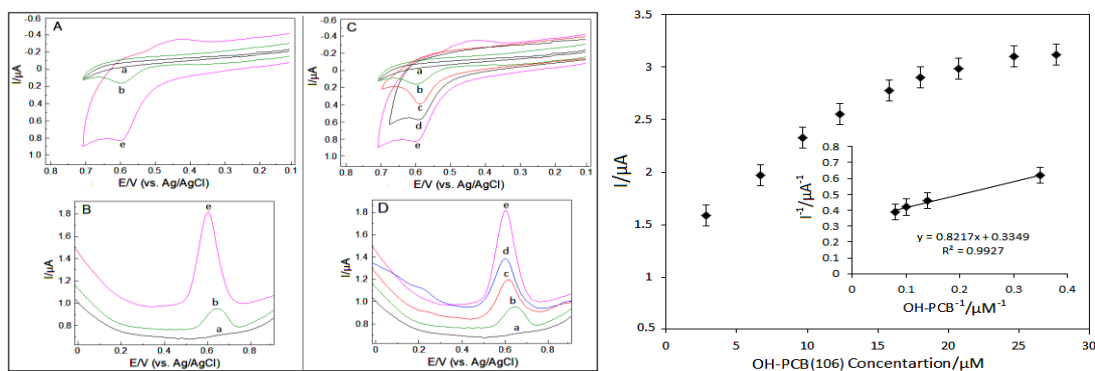


Figure 4: Comparison of cyclic (A and C) and squarewave (B and D) voltammograms in presence and absence of 2.8 μM OH-PCBs at different types of electrodes: GCE (curve b), GO/GCE (curve c), *Tyr*/GO/GCE (curve d) and *Tyr*-ZnO/GO/GCE (curve e). Curve a represents the background measurement in the absence of OH-PCBs; Calibration curve of *Tyr*-ZnO/GO/GCE for successive addition of OH-PCBs (2.8, 6.7, 9.7, 12.3, 15.8, 17.98, 20.7, 24.65, and 27.65 μM) in pH 7.2.

It can be seen from Figure 4 that the response current is linear with OH-PCBs concentration over a range from 2.8 to 17.98 μM , indicating that enzyme catalytic reaction of *Tyr* is first-order reaction. The detection limits were calculated and was found to 0.15 μM . However when the concentration of OH-PCBs is further increased from 17.98 to 27.65 μM , the current increases slowly and the enzyme reaction shows a transition from first to zero-order showing a characteristic of the Michaelis-Menten kinetic mechanism calculated according to the electrochemical version of the Lineweaver-Burk equation [6] which gives the K_M^{app} value of 17.70 μM .

6.3 Conclusions

In summary, we have developed a *Tyr*-ZnO/GO/GCE biosensor based on the use of graphene oxide platform amplification for immobilization of hybrid composed out of tyrosinase and ZnO QDs for the detection of OH-PCBs. The scanning electron microscopic images and UV-Vis spectroscopic analysis demonstrated the adsorption of tyrosinase with low isoelectric point on the positively charged surface of ZnO QDs by electrostatic attractions retain its bioactivity to a large extent and exhibits a good analytical performance for the detection of OH-PCBs. Thus by combining the specific properties such high catalytic activity of tyrosinase and large surface area of ZnO QDs, the synergistic effects of composite hybrid increased the amounts of OH-PCBs present at the electrode surface and resulting in an increase of the electrochemical responses of fabricated biosensor. In addition, the suggested sensing platform exhibits good reproducibility showing a great potential for rapid, cost-effective and becomes on-field pragmatic tool for convenient detection of other phenolic endocrine disruptors in environmental matrices.

6.4 References

- [1] A. K. Geim, K. S. Novoselov, Nat. Mater. 6 (2007) 183.
- [2] C. L. Y. Su, X.Y. H. L. Xia, Y. J. Wang, Sen. Actuators B: Chem. 149 (2010) 427.
- [3] F. F. Zhang, X. L. Wang, S. Y. Ai, Z. D. Sun, Q. Wan, Z.Q. Zhu, Y. Z. Xian, L. T. Jin, K. Yamamoto, Anal. Chim. Acta 519 (2004) 155-160.
- [4] H. Li, K. G. Drouillard, E. Bennett, G. D. Haffner, R. J. Letcher. Environ. Sci. Technol. 37(2003) 832.
- [5] N. Duran, M. Rosa, A. D'Annibale, L. Gianfreda, Enzyme Microb. Tech. 31 (2002) 907.
- [6] R. A. Kamin, G. S. Willson, Anal. Chem. 52 (1980) 1198.

VII. Fullerene- β -cyclodextrin conjugate based electrochemical sensing device for ultrasensitive detection of *p*-nitrophenol

7.1 Objectives

Fullerenes are considered as powerful building blocks in material and biological sciences due to their unique photochemical, electro-physical and electrochemical properties. However, due to the lack of solubility in polar solvents and the formation of aggregates in aqueous solution, their applications are rather limited. Among fullerenes, C_{60} is a ball-shaped conjugated electroactive molecule belonging to the carbon nanocluster family. Fullerene C_{60} is capable of accepting up to six electrons when dissolved in liquid electrolytes. This process can be generated electrochemically leading to potential applications as electron acceptor in electrochemical devices [1]. The reduced C_{60} films behave as diodes with pronounced current rectifying character and hence behave as individual microelectrodes leading to lowering of the peak potential along with enhancement in the peak currents and as a result improving the selectivity and sensitivity of the sensing device.

Cyclodextrins (CDs) belong to the family of bucket-shaped oligosaccharides macrocyclic molecules consisting of (+)-glucopyranose units. The depth of the cavities of CDs (α , β and γ) is 0.57, 0.78 and 0.95 nm, respectively. The inner side of the cavities is hydrophobic and outer side is hydrophilic facilitating the ability of CDs to act as host for guest molecules [2]. Once the inclusion compound is formed, the stability of the guest molecules increases due to binding forces (van der Waals attractions, hydrogen bonding, hydrophobic attractions, etc.) between the host (CDs) and guest molecules.

In order to combine the electrocatalytic properties of fullerenes and the inclusion capabilities of cyclodextrins, a number of conjugates have been synthesized [3]. In the present study a conjugate of fullerene (C_{60})- β -cyclodextrin was prepared as reported [4] and was characterized by NMR, UV-Vis spectroscopy, scanning electron microscopy and electrochemistry. The electrocatalytic properties of the conjugate were tested towards an aromatic nitro compound, i.e. *p*-nitrophenol.

The analysis of aromatic nitro compounds in natural water and effluents is of major importance for environmental control and hence these compounds have been included in the environmental legislation. In particular, *p*-nitrophenol (PNP) is one of the nitrophenols cited in the list of Priority Pollutants of the U.S.A. Environmental Protection Agency (EPA) due to its toxicity (carcinogen, teratogenic and mutagenic) and persistence and hence its application should be strictly controlled and supervised. Unfortunately, PNP is still widely used as intermediate in the production of parathion insecticide and will be inevitably released into the environment. Based on all these aspects, there is a need to develop simple and reliable sensing devices for the determination of trace amounts of PNP in the environment.

Thus, the present study involves the synthesis and use of fullerene (C_{60})- β -cyclodextrin conjugate for fabrication of an electrochemical device for the ultrasensitive detection of PNP (β -CD is selected as the molecular size of PNP is 0.67 nm [5, 6]). The sensitivity of the developed device is due to the synergetic effect which involves the electrocatalytic effect of fullerene (C_{60}) and the host guest relationship of β -cyclodextrin with PNP.

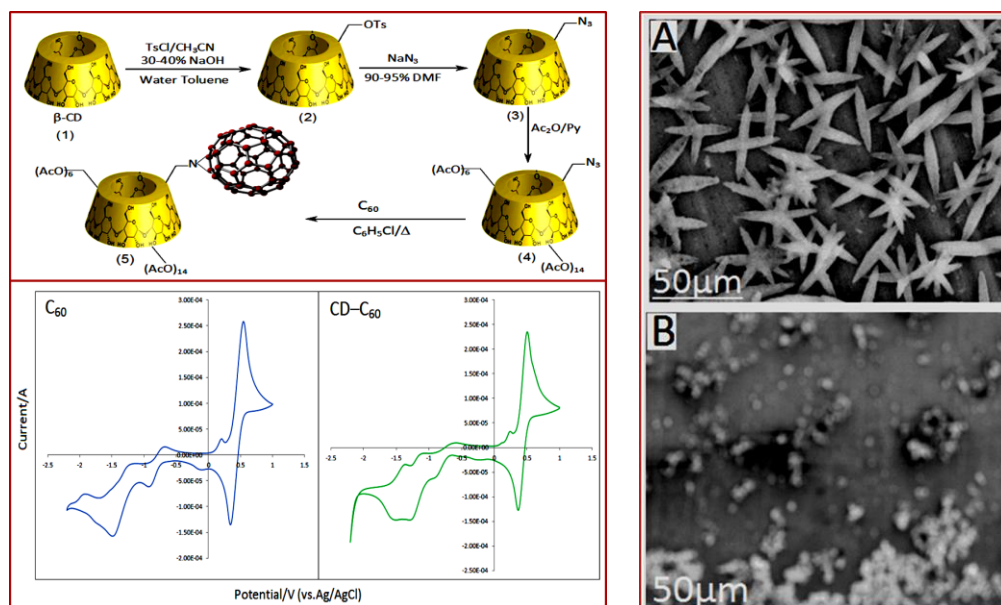


Figure 1: Synthesis of a fullerene (60)– β -cyclodextrin conjugate and the electrochemical characterization of C_{60} and fullerene (60)– β -cyclodextrin conjugate (CD– C_{60}) in $0.1 \text{ molL}^{-1} \text{ Bu}_4\text{NClO}_4$; SEM images of C_{60} (A) and fullerene (60)– β -cyclodextrin conjugate (B).

The fabrication of sensor involves dropping $8 \mu\text{L}$ of CD– C_{60} dissolved dichloromethane onto the surface of GCE using a microsyringe and dried at room temperature. The CD– C_{60} /GCE was scanned in the range of 1.0V to -2.5V in an acetonitrile solution containing $0.1 \text{ molL}^{-1} \text{ Bu}_4\text{NClO}_4$ using ferrocene as internal redox indicator for 15 scans until four electron reversible steps are obtained (Figure 1). The later confirms a successful immobilization of CD– C_{60} at GCE. A C_{60} /GCE was prepared and electrochemically screened. The CD– C_{60} /GCE and C_{60} /GCE was also characterized by scanning electron microscopy (Figure 1).

7.2 Results and Discussion

The electrochemical characterization of the CD– C_{60} /GCE sensing device was carried out by electrochemical impedance spectroscopy (EIS) and cyclic voltammetry (CV) (Figure 2). The developed CD– C_{60} /GCE sensing device was applied for the determination of PNP. The cyclic voltammetric behaviour of PNP was scanned in the range of potential -1.5 to $+1.5\text{V}$ in a solution of an acetate buffer pH 5 depicted in Figure 2A. It is observed that PNP yields one reduction peak R_1 resulted from an irreversible reduction of the nitro group to give the corresponding hydroxylamine species. In addition a pair of well-defined redox peaks (R_2 and O_1) was obtained during the second scan due to quasi-reversible behavior of hydroxylamine to its derivative as reported [7]. The squarewave voltammograms obtained with increasing amounts of PNP show that the peak current increases linearly with increasing PNP concentration over the range of $2.8 \times 10^{-9} \text{ molL}^{-1}$ to $4.2 \times 10^{-7} \text{ molL}^{-1}$ (Figure 2B). The detection limit (LOD) was calculated to be $1.2 \times 10^{-9} \text{ molL}^{-1}$ which is lower than the reported electrochemical methods for the detection of PNP

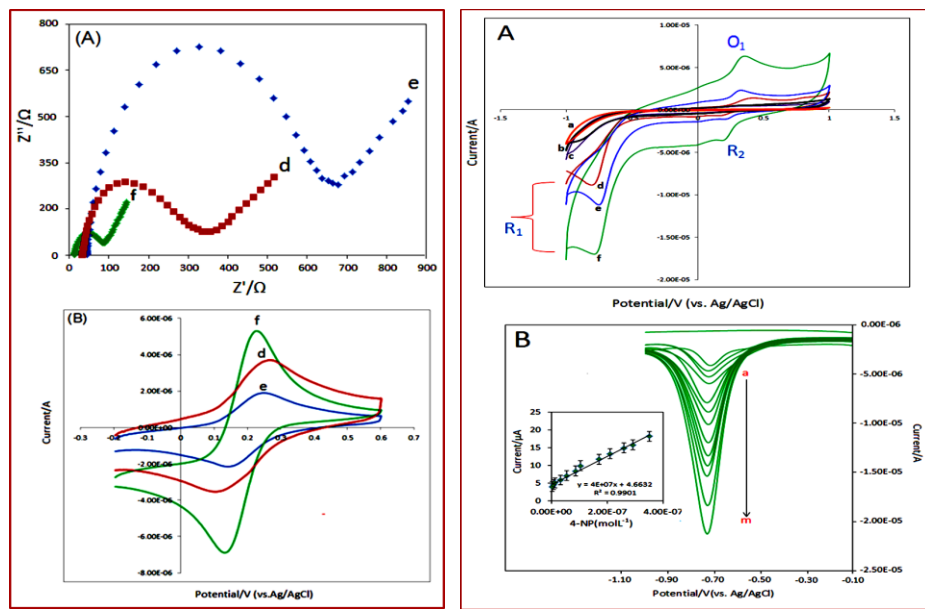


Figure 2: Nyquist plots (A) and cyclic voltammograms (B) obtained at GCE (curve *d*), C_{60}/GCE (curve *e*) and $CD-C_{60}/GCE$ (curve *f*) in 1.0 mM $K_3[Fe(CN)_6]$; Figure 4: (A) Cyclic voltammetric behavior obtained in the absence (curve *a–c*) and the presence (curve *d–f*) of 1.2×10^{-6} molL⁻¹ PNP at GCE; blank C_{60}/GCE ; blank $CD-C_{60}/GCE$; 1.2×10^{-6} molL⁻¹ PNP at GCE; C_{60}/GCE and $CD-C_{60}/GCE$, scan rate 20 mVs⁻¹; (B) Linearity of squarewave voltammetric peak current of different concentrations of PNP (2.8×10^{-9} to 4.2×10^{-7} molL⁻¹) at $CD-C_{60}/GCE$. Inset a calibration graph represents the variation of current with the concentration of PNP. The error bars shows the standard deviation obtained for three separate experiments.

7.3 Conclusion

In this study, we have synthesized a fullerene (60)- β -cyclodextrin conjugate fully characterized by spectroscopy and electrochemical techniques. This conjugate was successfully immobilized on the surface of a glassy carbon electrode to develop a $CD-C_{60}/GCE$ sensing device for the detection of *p*-nitrophenol. The developed device shows high electrocatalytic analytical performance due to synergetic of C_{60} (microelectrodes) and β -cyclodextrin (acceptor–host system) for the sensing of *p*-nitrophenol. The calculated detection limit of 1.2×10^{-9} molL⁻¹ for *p*-nitrophenol using the developed device is lower than other reported values attained by electrochemical sensors. The fabricated device shows a great potential for rapid, cost-effective and becomes on-field pragmatic tool for convenient detection of *p*-nitrophenol in environmental matrices.

7.4 References

- [1] M. S. Dresselhaus, G. Dresselhaus, P. C. Eklund, Science of Fullerenes and Carbon Nanotubes; Academic: San Diego, 1996.
- [2] J. Szejtli, Chem. Rev. 98 (1998) 1743.
- [3] T. Anderson, K. Nilsson, M. Sundahl, G. Westman, O. Wennerstro, J. Chem. Soc. 8 (1992) 604.
- [4] F. Giacalone, F. D'Anna, R. Giacalone, M. Gruttadauria, S. RIELA, R. Noto, Tetrahedron Lett. 47 (2006) 8105.
- [5] L. Xiaohong, Z. Baowei, Z. Kun, H. Xuekui, Chin. J. Chem. Eng. 19 (2011) 6.
- [6] J. Szejtli, Cyclodextrins and their Inclusion Complex, Akademiai Kiado, Budapest, 1982.
- [7] T. Alizadeh, M. R. Ganjali, P. Norouzi, M. Zare, A. Zeraatkar, Talanta 79 (2009) 1197.